International Journal of Applied Engineering Research ISSN 0973-4562 Volume 15, Number 9 (2020) pp. 891-905

The Use of Tannery Solid Waste in the Production of Building Bricks

S.A. Ghonaim[1], M.F. Abadir[2], I.A.Ghoneim[3], Sh.K. Amin[4,*]

[1]*The Faculty of Engineering and Technology, Badr University (BUC), Cairo, Egypt.*

[2] *The Chemical Engineering Department, Faculty of Engineering, Cairo University, Egypt.*

[3]*The Science and Technology Centre for Excellence (STCE) at the NOMP, Egypt.*

[4]*Chemical Engineering and Pilot Plant Department, Engineering Research Division, National Research Centre (NRC), Giza, Egypt. (Affiliation ID: 60014618).*

Abstract

Tannery solid waste represents one of the burdensome environmental problems owing to the large quantities of discarded material besides the toxicity of the sludge. Experiments were performed to assess the possibility of using tannery solid waste obtained by drying the tannery sludge from The Rubiky leather city in Badr City (Egypt) in the preparation of clay bricks. This endeavor has a dual purpose: First, it makes use of an environmental unfriendly waste and second, it decreases the amount of clay used in the process. A third advantage may pop out from amelioration in the bricks properties or a decrease in the energy required for firing. Raw materials were characterized for their chemical and mineralogical composition using XRF and XRD respectively; the particle size distribution of both clay and tannery waste was assessed by sieving. Mixtures were prepared by mixing up to 10% waste with clay. Brick specimens for each mixture were molded, dried then fired. Tests performed on the wet mixes showed that waste addition caused an increase in drying shrinkage up to 10% addition. A slightly favors increase in the dry compressive strength by the addition of waste up to 10%. On firing for 3 hours at temperatures ranging from 700 to 850 °C the percent boiling water absorption as well as apparent porosity regularly increased on waste addition associated with a decrease in bulk density and hence the weight of produced bricks. The effect of firing temperature on compressive strength is not remarkable whereas the addition of tanning waste causes a steady decrease in strength; the values of strength are compared to the minimum allowable strength according to ASTM C62/2017 (8.7MPa). It was concluded that the tannery waste can be added to bricks up to 5% level with a firing temperature as low as 700ºC.

Keywords: Clay bricks, Tannery waste, Specifications.

1. INTRODUCTION

Clay brick is one of the oldest and most durable building materials used by mankind. The brick manufacturing technique is: Mixing clay with water and some ingredients then going through molding, drying and burning at temperatures between the 800 – 1000ºC range. Due to the diversity of the brick composition, researchers have been used different types of waste in fired clay bricks, even in high percentages [1; 2]. One of The most commonly used wastes are various types of fly ash [3], PVB-foils, sewage sludge [4], sawdust [5], kraft pulp residue [6], recycled paper [7], rubber [8], limestone dust [9], cigarette butts [10], rice hulls and husk [11], rice straw [12], grass [13], cement dust (a waste produced by the cement industry) [14] and many other industrial and domestic wastes. The utilization of these wastes plays an important role that helps in reducing the negative effects of their disposal process. However, the potential wastes can only be recycled if the properties and the environmental pollutant of the brick new manufacturing meet with the specific requirements and align with the relevant standard. As, Tannery solid waste disposition through dumpfilling has been contaminate soil, about 100-150 kg of sludge is generated per ton of hides/skins processed [15]. The aim of this paper is to assess the possibility of using tannery solid waste in the production of clay bricks. In this respect, the only investigation carried out for using tannery sludge in clay bricks making was published by Juel et al. [16] who used the sludge as mixing fluid instead of water and could obtain samples with reasonable mechanical properties. In their work, they failed however to interpret the different results obtained. The recent work of Amsayazhi et al. [17] was devoted to the preparation of cement bricks rather than clay bricks using tannery sludge as a mix component.

**** Corresponding Author:*** *Prof. Shereen Kamel Amin, Research Professor.*
E-mail : dr.shereenkamel@hotmail.com; sheren51078@yahoo.com

2. MATERIALS AND EXPERIMENTAL TECHNIQUES

2.1 Introduction

In this paper, experiments were performed to assess the possibility of using tannery solid waste obtained by drying the tannery sludge from The Rubiky leather city in Badr City (Egypt) in the preparation of clay bricks. This endeavor has a dual purpose: First, it makes use of an environmental unfriendly waste and second, it decreases the amount of clay used in the process. A third advantage may pop out from amelioration in the bricks properties or a decrease in the energy required for firing.

2.2 Raw Materials

Two types of raw materials were used in this work:

- The first consists of desert clay which is commonly used in fired clay brick industry. It was obtained from the "Egypt Brick Factory" located in 15th May City.
- The second part consists of tannery solid waste obtained by drying the tannery sludge from The Rubiky Leather City, Badr City in Egypt

2.3 Characterization of Raw Materials

The raw materials were subjected to the following analyses:

2.3.1 Chemical Analysis (XRF)

X–ray fluorescence spectrometry (XRFS) is a method of elemental analysis that assesses the presence and concentration of various elements by measurement of secondary X–radiation from the sample that has been excited by an X–ray source.

Classically elements from the heaviest down to atomic number 9 (F) can be determined at levels of a few mg / kg (ppm). Newer developments with wavelength dispersive spectrometers (WDXRF) allow the determination some of the ultra low atomic number elements including (O).

XRF analyses were run on a AXIOS, panalytical 2005, Wavelength Dispersive (WD–XRF) Sequential Spectrometer, which is installed at Natural Research Center – Preparation and Chemical Analysis using X–ray fluorescence Department.

2.3.2 Mineralogical Analysis (XRD)

X–Ray diffraction analysis differs from XRF in that it identifies, in a qualitative (or semi-quantitative) way, the phases present in the analyzed material rather than the elements.

For X–Ray diffraction study, the sample was split into two aliquots, one for bulk mineral analysis and the other for clay analysis. The aliquot for bulk mineral analysis was finely ground (-200 mesh), mounted randomly on an aluminum holder, and analyzed by a BRUKUR D_8 ADVANCED COMPUTERIZED X–Ray Diffractometer apparatus (At the Center Metallurgical Research and Development Institute) with mono–chromatized Cu K_α radiation, operated at 40 kV and 40 mA. The diffractograms were used to provide back ground information on the bulk mineralogy of the sample, and particularly to estimate the relative abundance of the non–clay minerals in the sample.

In the X–Ray Diffraction a collimated beam of X rays, with a specified wave length (λ) is incident on a specimen and diffracted by an angle (2θ) by the crystalline phases in the specimen according to Bragg's Law:

$$\lambda = 2d.\sin\theta \quad (1)$$

Where (d) is the spacing between atomic planes in the crystalline phase (nm). The intensity of the diffracted X rays is measured as a function of the diffraction angle and the specimen's orientation. The diffraction pattern is used to identify the specimen's crystalline phases [18; 19].

2.3.3 Thermal Analysis (TGA and DTG)

By thermal analysis is meant a set of analyses that rely on the physico–chemical changes that take place upon heating a material. The three principal thermo–analytical techniques are differential thermal analysis (DTA), thermo–gravimetry analysis (TGA) and derivative thermo–gravimetry (DTG). These terms were first adopted by the International confederation for Thermal Analysis [20].

DTA curves reveal all energy changes occurring in a sample on heating. TGA and DTG curves reveal only weight changes and their time derivative, occurring on heating (due to decomposition or oxidation) and therefore yield more limited information than DTA. Comparison of DTA and TGA, or even better, DTG curves immediately indicates which reactions relate to decomposition or oxidation. The usual criterion for DTA is peak temperature but, since this is dependent on many factors such as heating rate, sample size, particle size and distribution, etc., a better reference point is the extrapolated onset which is near the commencement of the reaction [20].

TGA and DTG were recorded on equipment "NETZSCH STA 409 C/CD", (Installed at Center Metallurgical Research and Development Institute).

2.3.4 Screen Analysis

In order to determine the particle size distribution of raw materials, the standard sieving procedure described by ASTM D 422 / 2007 was used [21]. It consists mainly of a sensitive digital balance (± 0.01 g), and a standard set of sieves installed on a laboratory scale shaker, with both lateral and vertical motions, accompanied with a jarring action in order to keep the sample moving continuously over the surface of the sieve. The sieves used are in compliance with ASTM E 11 / 2009 [22]. The cumulative analyses are reported then represented on a semi logarithmic graph [23].

2.4 Preparation of unfired Brick Samples

The tannery solid waste in form of powder obtained by drying tannery sludge was used as additive to clay as the basic materials in the fired clay brick manufacturing, in percentage of weight starting from 0 % till 10 %, increasing by 2 %. This way, six mixtures were prepared. These mixtures were mixed on dry basis for 10 minutes for each sample. Shaping of the bricks was carried out as follow:

a) Cubic brick specimens of approximate dimensions 50×50×50 mm^3, were molded by semi-dry pressing using a laboratory hydraulic press under uniaxial pressure of 20KN force (Corresponding to a pressure of 6MPa) , with 15 % water addition.

b) Brick specimens were dried on three steps using a laboratory dryer. The first step was at 50°C for 24 hours, then at 80°C for three hours, then at 110 °C for another three hours. This was made to ensure slow release of water from the bodies.

c) Each brick sample consists of three specimens for each mixture.

2.5 Testing of unfired brick samples

2.5.1 Determination of Shrinkage for Prepared Samples

The linear and volume shrinkage of unfired and fired brick samples were measured according to ASTM standard C 326/2009(R2018) [24]. The purpose of this test is to obtain values of both linear and volume shrinkage after drying and firing of clays or bodies or both, under various processing conditions to enable designers to determine the proper size of mold or die so as to produce a predetermined size of fired ware.

Drying shrinkage takes place during the constant rate period due to the evaporation of layer water during drying. On the other hand, the firing shrinkage takes place on firing due to sintering and possible vitrification of the fired bodies.

This shrinkage is easily determined by measuring the original length of the molded bricks before and after drying and its length after firing by using a vernier caliper.

The linear drying shrinkage, expressed as a percent, was calculated as follows:

$$\text{L.D.S.\%} = \frac{L_i - L_d}{L_i} \times 100 \quad (2)$$

Where:

L_i = Greatest side length before drying (original length) mm

L_d = Greatest side length after drying mm

2.5.2 Determination of green Compressive Strength [ASTM C 67 / 2017] [25]

The test specimens consist of unfired dried brick samples subjected to compressive loading in a UTM. The load is applied at a uniform rate so that the duration of its application lies between 1 and 2 minutes. The green compressive strength of each specimen (reported to the nearest 0.01 MPa) is calculated as follows:

$$\sigma_C = \frac{W}{A} \quad (3)$$

Where:

σ_C = Compressive strength of specimen MPa

W = Maximum load, indicated by the testing machine N

A = Average of the cross sectional areas of the upper and lower bearing surfaces of the specimen mm^2

2.6 Firing of Building Brick Samples

Brick specimens were fired using a laboratory muffle furnace to different three temperatures (700°C, 750°C, and 800°C), for one hour soaking time, and total firing time of 3 hours. Heating rates were chosen to be as close as possible to industrial conditions.

The firing schedule can be described as follows:

i. The temperature was increased from room temperature to 400 °C in 1 hour.

ii. The temperature was increased from 400°C to 600°C in 1 hour in order to provide a slow escape of organic impurities and combined water so as to prevent crack formation.

iii. The temperature was increased from 600°C to the maximum firing temperature with 1 hour soaking time.

The dimensions of the fired bricks were determined using a vernier caliper both before and after firing. Also, the mass of bricks was determined both before and after firing using a digital balance displaying its readings up to 0.01 g. accuracy.

2.7 Testing of Fired Brick Samples

2.7.1 Determination of Loss on Ignition

The loss on ignition test is designed to measure the amount of moisture or impurities lost when the sample is ignited under the firing conditions. The loss on ignition of fired tile samples was measured according to ASTM standard D 7348/2013 [26]

The LOI is easily determined by weighing the molded bricks after drying, then it's re–weighing after firing. The loss on ignition, expresses as a percent, was calculated as follows:

$$\text{LOI \%} = \frac{m_d - m_f}{m_d} \times 100 \quad (4)$$

Where:

m_d = Mass of dried brick sample g.

m_f = Mass of fired brick sample g.

2.7.2 Determination of Firing Shrinkage

In order to know the linear and volume firing shrinkage of each specimen after firing at different values firing temperature for 1 hour soaking time, and percent waste addition, the method which is described in section (2.5.1) is used [ASTM C 326/2009 (R2018)]. The percent firing shrinkage is calculated from the expression:

$$\text{L.F.S.\%} = \frac{L_d - L_f}{L_d} \times 100 \quad (5)$$

Where:

L_i = Greatest side length before firing (dry length) mm

L_d = Greatest side length after firing mm

2.7.3 Determination of Cold and Boiling Water Absorption, and Saturation Coefficient

Cold and boiling water absorption were calculated and reporting done as recommended in ASTM C 67 / 2017:

(a) Cold Water Absorption:

This test is essentially carried out by first weighing the dry cold specimen which is then immersed in distilled water for 24 hours. The specimen is then removed and its surface wiped with a damp cloth. The specimen is then weighed again and the percent cold water absorption determined from the expression:

$$\text{C.W.A.\%} = \frac{m_{cw} - m_d}{m_d} \times 100 \quad (6)$$

Where:

m_{cw} = Saturated mass after immersion in cold water g.

m_d = Original dry mass g.

(b) Boiling Water Absorption:

This test is carried out on the same specimens used for the cold water absorption test. These specimens are immersed in distilled water that is heated to boiling. The specimens are then allowed to remain 5 hours in boiling water, after which they are allowed to cool to room temperature by natural convection. The specimen is then removed and its surface wiped with a damp cloth. The specimen is then weighed again and the percent boiling water absorption determined from the expression:

$$\text{B.W.A.\%} = \frac{m_{bw} - m_d}{m_d} \times 100 \quad (7)$$

Where:

m_{cw} = Saturated mass after immersion in boiling water g.

m_d = Original dry mass g.

(c) Saturation coefficient:

This parameter simply measures the ratio between the cold and boiling water absorption. It is related to the size of pores in the following way: Gases entrapped in small pores will resist the flow of cold water; upon boiling, these gases will escape allowing water to fill these pores. In case of large pores, the surface tension of gas bubbles does not appreciably impede the flow of water into these pores. That is why a saturation coefficient close to unity denotes the presence of large pores. The saturation coefficient is usually calculated from the following expression:

$$\text{S.F.} = \frac{m_{bw} - m_d}{m_{cw} - m_d} \quad (8)$$

2.7.4 Determination of Apparent Porosity, Bulk Density, and Specific Gravity [ASTM C 373/1988 (Reapproved 2006)] [27]

This standard allows for the determination of the above mentioned parameters from one test that includes weighing a dry specimen, then immersing in boiling water for 5 hours and leaving the specimen to cool while in water. The specimen is then removed from water, its surface wiped by a wet cloth then weighed while saturated with water.

The apparent porosity is calculated from the following expression:

$$P\% = \frac{m_{bw} - m_{df}}{V_d} \times 100 \quad (9)$$

Where:

m_{cw} = Saturated mass after immersion in boiling water g.

m_{df} = Original dry mass of fired specimen g.

V_{df} = dry volume of fired specimen (Geometric volume)cm^3

On the other hand, the bulk volume is calculated by dividing the dry mass of the fired specimen by its geometric volume:

$$\rho_b = \frac{m_{df}}{V_{df}} \ g.cm^{-3} \quad (10)$$

Finally, the apparent specific gravity indicates the ratio between the mass of the dried fired specimen and the apparent volume excluding its open connected pores. It is calculated from the expression:

$$\rho_b = \frac{m_{df}}{m_{df} - m_s} \quad (11)$$

Where,

m_s is the mass of the specimen while suspended in water (g.)

2.7.5 Determination of Compressive Strength of fired specimens [ASTM C 67 / 2017]

The test specimens consist of fired brick samples subjected to compressive loading in a UTM. The load is applied at a uniform rate so that the duration of its application lies between 1 and 2 minutes. The compressive strength is determined in the same way as was done for green samples by using equation (3).

3. RESULTS AND DISCUSSION

3.1 Characterization of Raw Materials

3.1.1 Chemical Analysis

The raw materials were subjected to chemical analysis determined as previously mentioned by XRF. The results are shown in Table (1).

Table (1): Chemical analysis of raw materials

Constituents, Wt %	Clay	Tannery Waste
SiO_2	53.39	2.03
Al_2O_3	14.30	0.2
$Fe_2O_3^{tot.}$	10.90	1.5
TiO_2	0.80	0.16
MgO	1.49	0.01
CaO	3.10	1.4
Na_2O	1.62	1.05
K_2O	1.26	1.29
P_2O_5	0.06	0.19
SO_3	0.90	1.62
Cl	0.43	9.99
Trace elements	0.364	0.02
L.O.I	11.34	80.40
Total	**99.95**	**99.86**

3.1.2 Mineralogical Analysis (XRD)

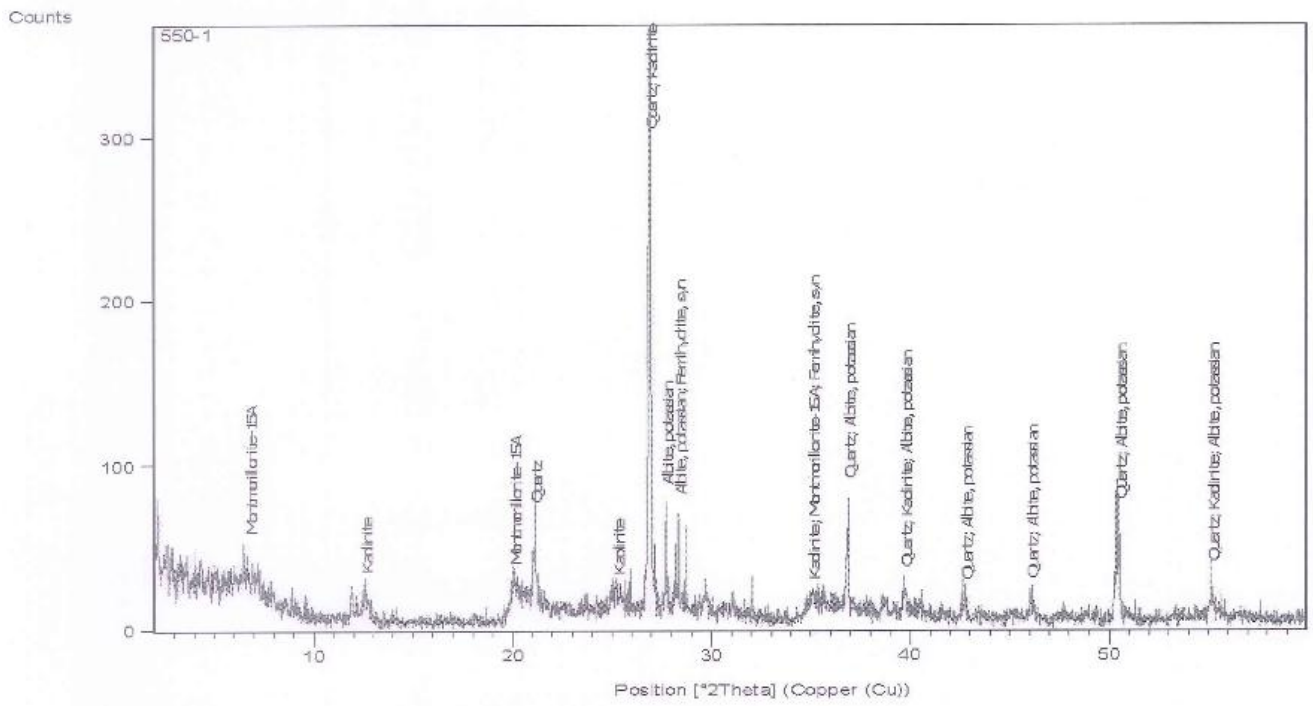

Fig (1) XRD Pattern for Clay

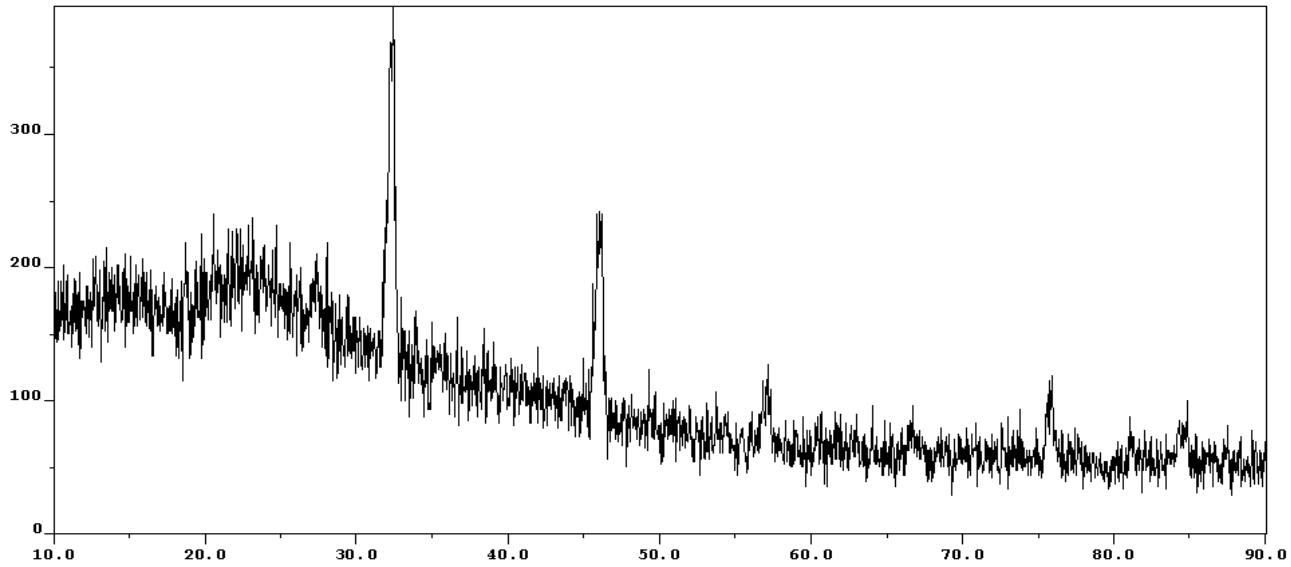

Fig (2) XRD Pattern for Tannery Solid Waste

The XRD pattern of clay shows that the main phases are kaolinite ($Al_2Si_2O_5(OH)_4$), montmorillonite ($(Na,Ca)_{0.33}(Al,Mg)_2(Si_4O_{10})$) and quartz ($SiO_2$). On the other hand, the XRD pattern for tannery waste powder only produced diffuse peaks at some diffraction angles. Table (2) shows the interpretation of these peaks [28; 29; 30].

Table (2): Phases present in tannery waste

2θ	Phase	Reference
32.3	NaCl	28
46	$FeCl_3$	29
57.6	$FeCl_3$	29
65.6	NaCl	28
76	$Ca_2Al_2SiO_7$	30

3.1.3 Thermal Analysis

Figure (3) reveals the TG/DTG pattern of a specimen of the clay used passing from 200 mesh sieve (74μm) performed at a rate of $10^oC.min^{-1}$ in air. The early losses in weight are due to moisture elimination and end at about 165°C. The slight loss in weight corresponding to the DTG peak extending from 250 to 300°C is probably due to oxidation of minor organic impurities present in clay. The main loss starting at about 400 and ending at 600°C denotes the dehydroxylation of the kaolinite and montmorillonite species present in clay. Actually, this peak extends to about 800°C whereby the total loss in weight reaches 12.9%, a figure close to that obtained for LOI (Table 1).

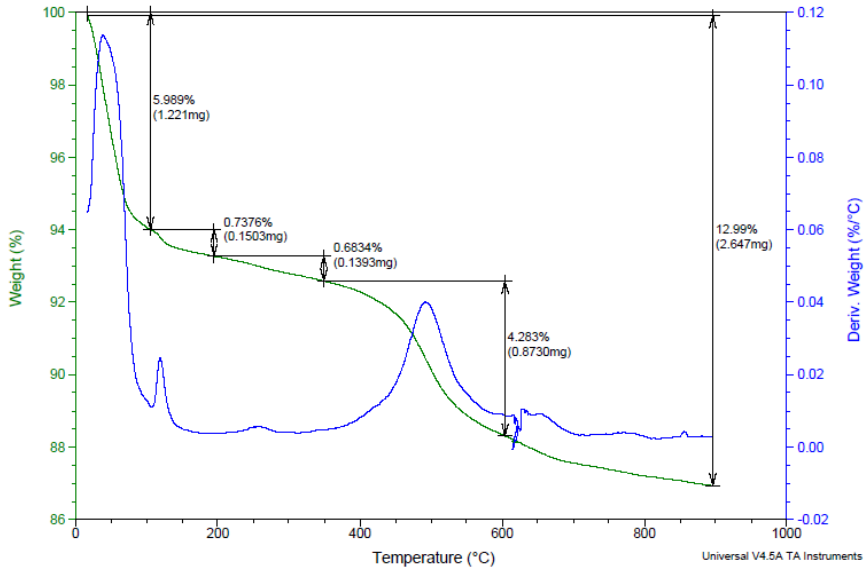

Fig (3) TGA Pattern for Clay

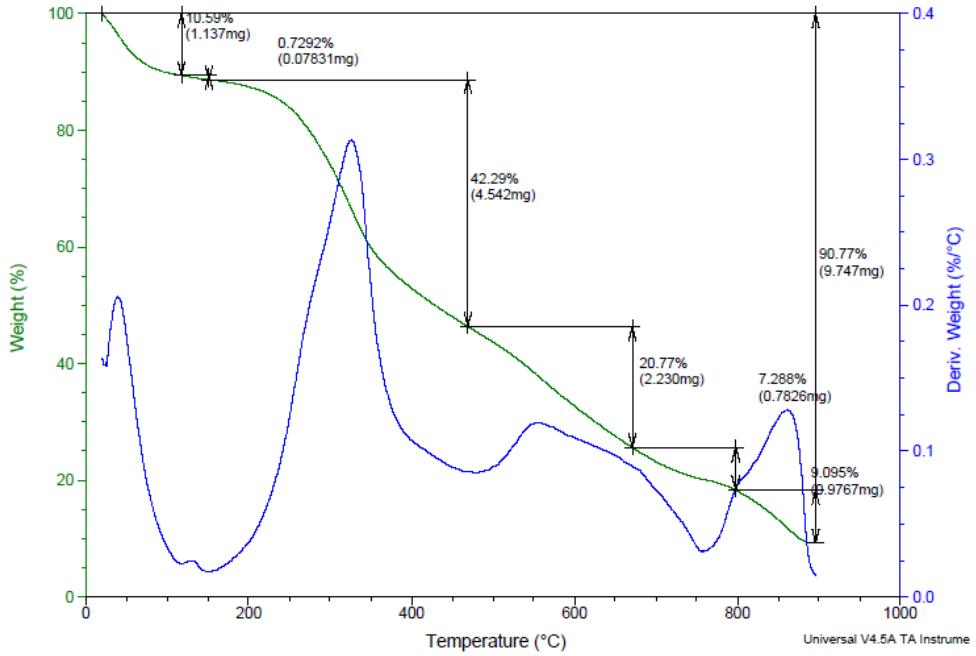

Fig (4) TGA Pattern for Tannery Solid Waste

The thermal analysis pattern for tannery waste powder is more complicated and shows a loss in weight due to moisture loss of more than 10%. The final loss in weight of the remaining dry powder at 900ºC reaches about 80.8%, a figure identical to the LOI mentioned in Table (1).

3.1.4 Screen Analysis

Figure (5) displays the screen analysis of the two materials used in this work. As can be deduced from that figure, clay is coarser in size than the tannery waste obtained from drying tannery sludge. Actually, the median particle size for clay is $D_{50} = 0.85\mu$m while it is 0.18μm for the waste.

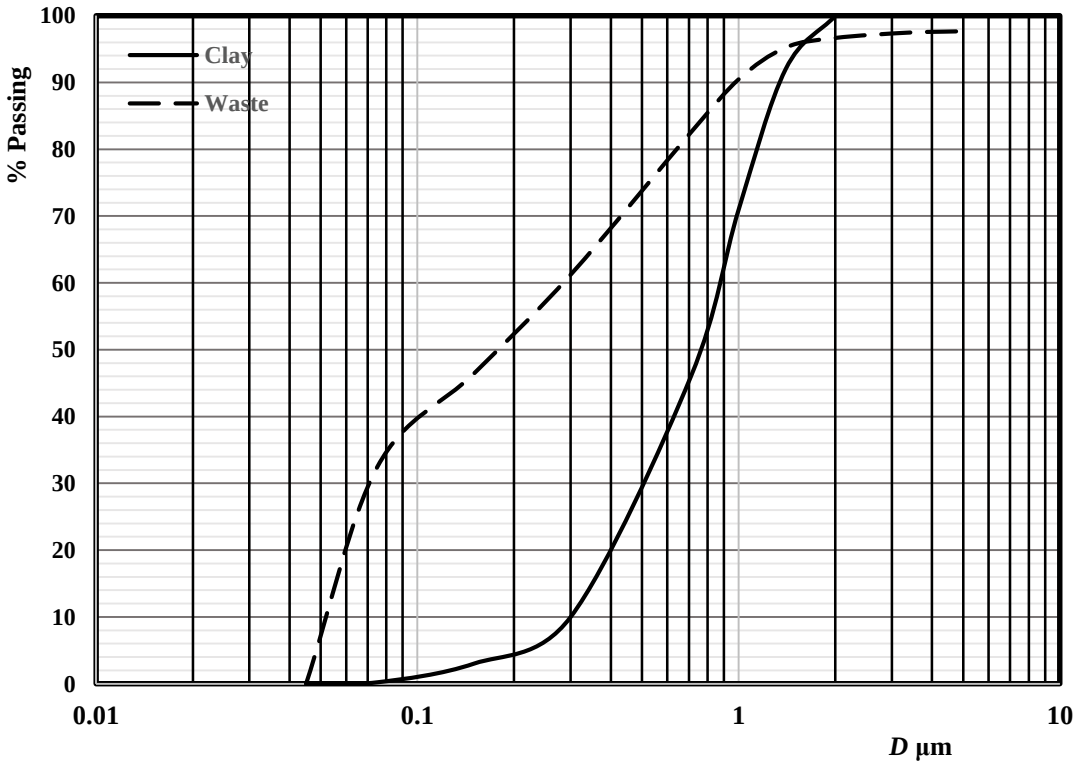

Fig (5) Cumulative screen analysis of raw materials

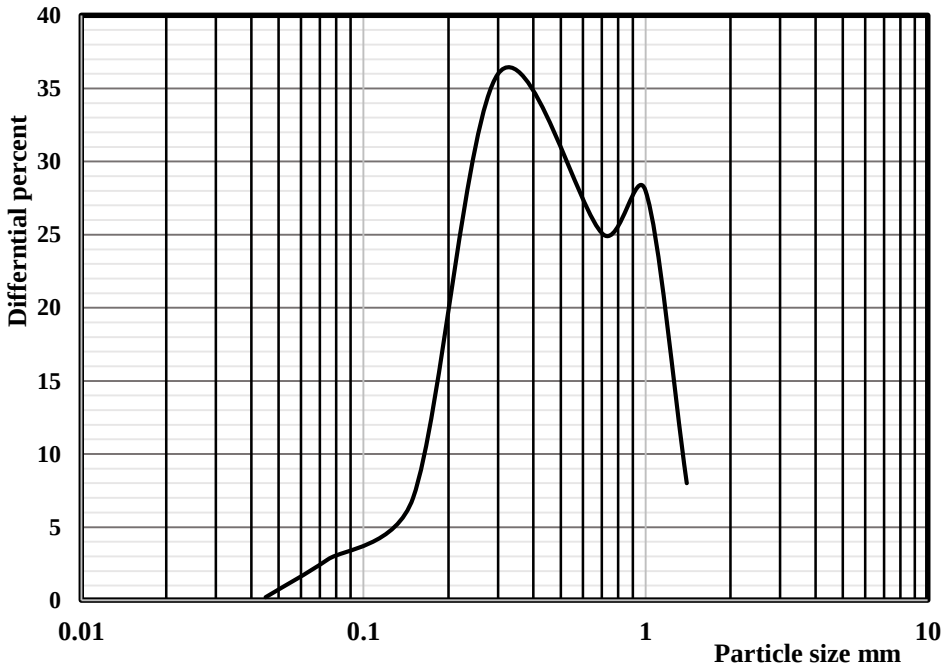

Fig (6) Differential screen analysis of clay

The bimodal distribution of the differential screen analysis of clay shown in Figure (6) indicates the presence of a moderate to appreciable amount of free silica [31].

3.2 Testing of Unfired Brick Samples

3.2.1 Determination of Shrinkage [ASTM C 326 / 2009 (R2018)]

As can be deduced from Figure (7), the addition of the waste to clay caused an increase in drying shrinkage, presumably because of the relocation of fine waste particles within the coarser particles of clay. This causes the total volume of the specimen to decrease. However, the magnitude of the shrinkage was not appreciable as the percent linear shrinkage remained constant up to about 4% addition at 0.08% then increased almost linearly to reach 0.53% at an addition level of 10%. One reason for the negligible shrinkage is the presence of an appreciable amount of free silica in clay. Actually, the presence of free silica was demonstrated by the bimodal nature of the differential particle size distribution in Figure (6).

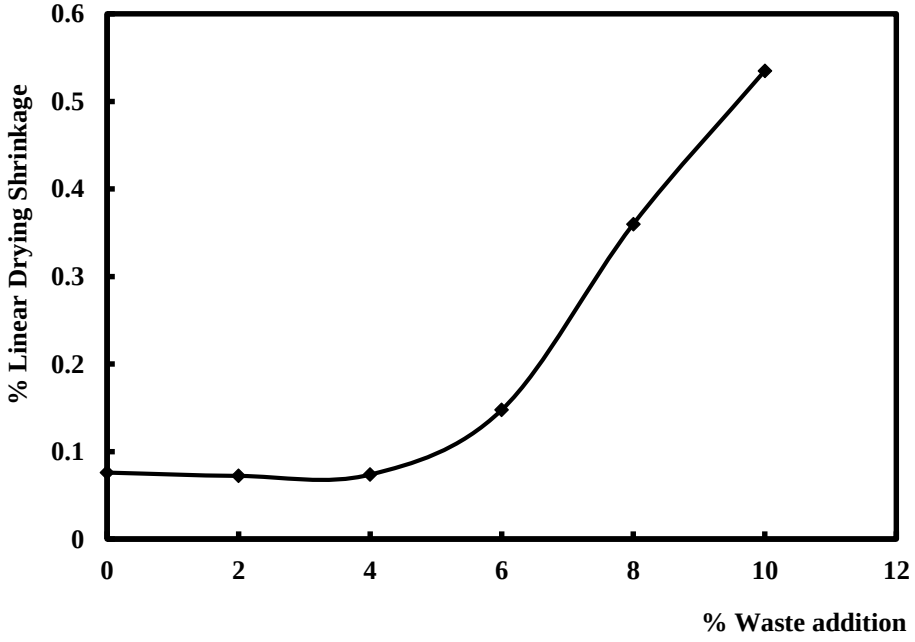

Fig (7) Effect of waste addition on linear drying shrinkage

3.2.2 Determination of Compressive Strength [ASTM C 67 / 2017]

Figure (8) represents the variation of green compressive strength as function of percent waste added. This figure reveals that the addition of waste slightly favors the green strength as its value increases from an initial value of 7.1MPa when no waste was added to reach 7.9MPa at 10% addition. It is believed that increased drying shrinkage is the reason for that behavior as particles get more compacted through shrinkage. This is emphasized by the increasing relation between green compressive strength and percent linear shrinkage illustrated in Figure (9).

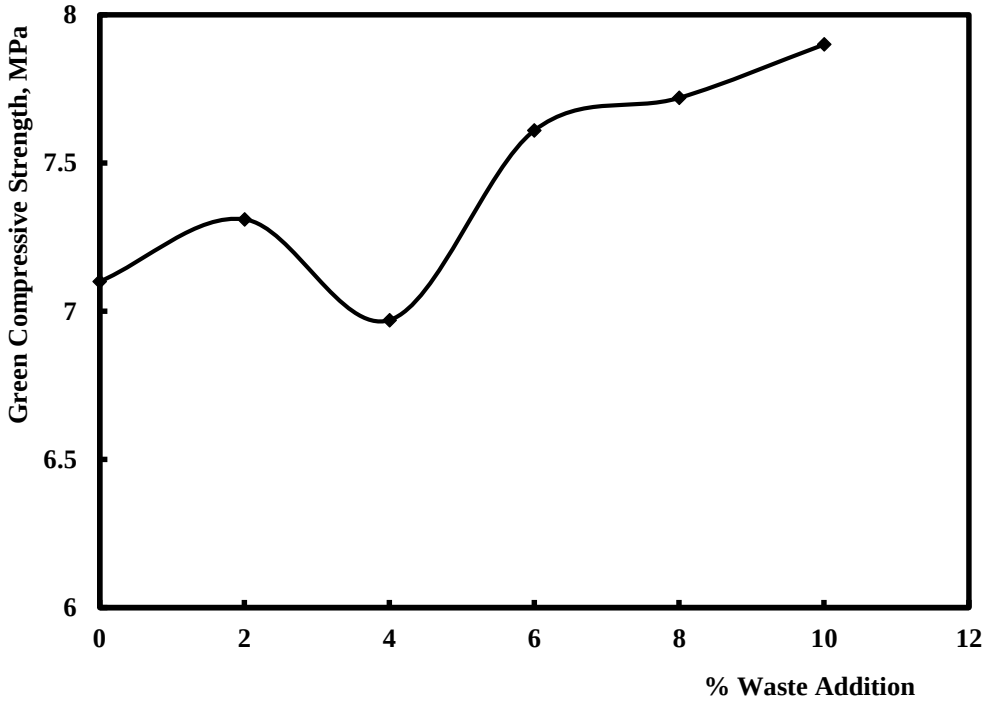

Fig (8) Effect of waste addition on green compressive strength

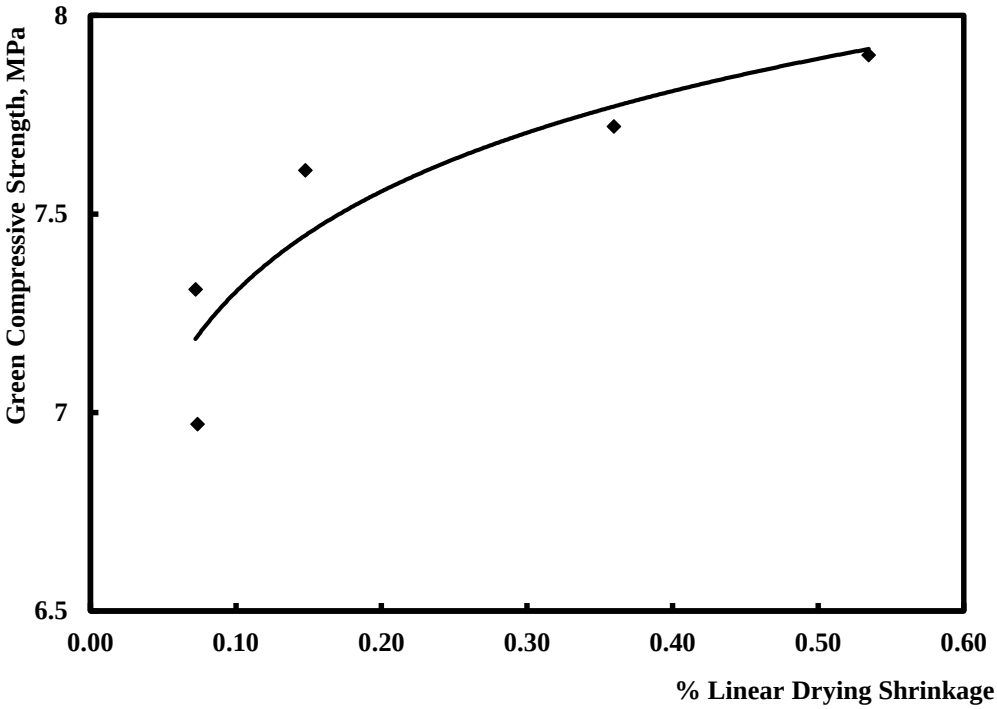

Fig (9) Relation between green compressive strength and linear shrinkage

3.3 Testing of Fired Brick Samples

As mentioned earlier the dried samples were subjected to firing at three different temperatures namely, 700, 750 and 800ºC. The different properties of fired samples were determined as function of both firing temperature and percent waste added.

3.3.1 Determination of Loss on Ignition [ASTM D 7348/2013]

The percent weight loss on firing, illustrated in Figure (10) reveals that the effect of percent weight addition on weight loss in firing is much higher than that of percent waste added. There doesn't seem to be any difference between the loss for samples fired at 750 or 800ºC.

It can be seen from Figure (3) that the net percent loss in weight of a dry specimen at 800ºC (Excluding the first two peaks corresponding to loss in moisture) = 6.2%. On the other hand, the loss in weight on firing for the waste at the same temperature = 80.8%. Therefore the theoretical loss in weight on firing to 800ºC can be predicted from the expression:

$$\% \text{ Loss} = 6.2(1 - x) + 80.8x \quad (12)$$

Where, x is the fractional amount of waste added.

Figure (10) shows a good agreement between the experimental results and the theoretical forecast at 800ºC.

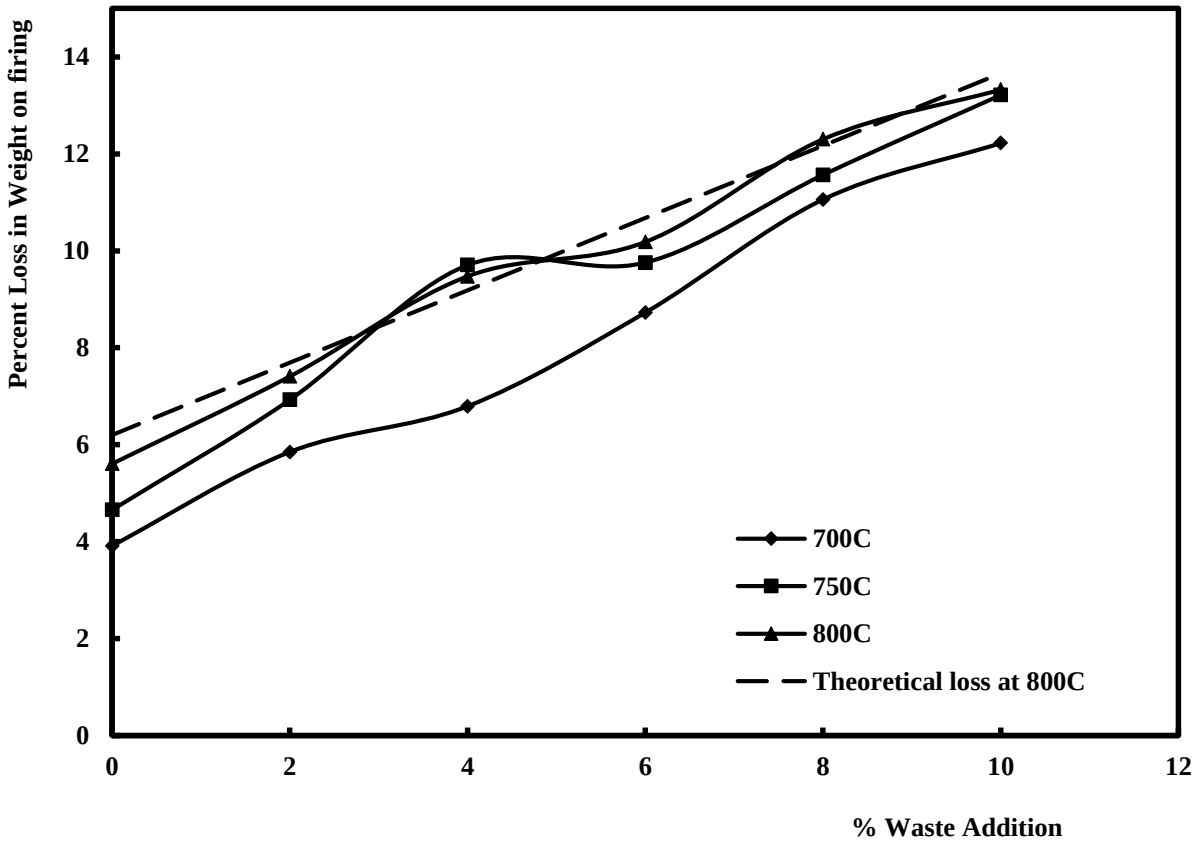

Fig (10) Effect of waste addition on loss on ignition of fired samples

3.3.2 Determination of Firing Shrinkage [ASTM C 326/2009 (R2018)]

Actually, the effect of either firing temperature or percent waste addition on the linear firing shrinkage was not appreciable. The values of that parameter fluctuated erratically between 0% and 1%. That is why these relations were not shown as plots.

3.3.3 Determination of water absorption and saturation coefficient [ASTM C 67/2017]

As can be seen from Figure (11), cold water absorption of fired samples increases with increased waste addition due to the creation of pores associated with the volatilization of the organic portions of the waste. On the other hand, an increase in firing temperature results in a decrease in water absorption due to initiated sintering.

A similar situation can be observed in Figure (12) for boing water absorption although the dependence on firing temeprature is less pronounced than in case of cold water.

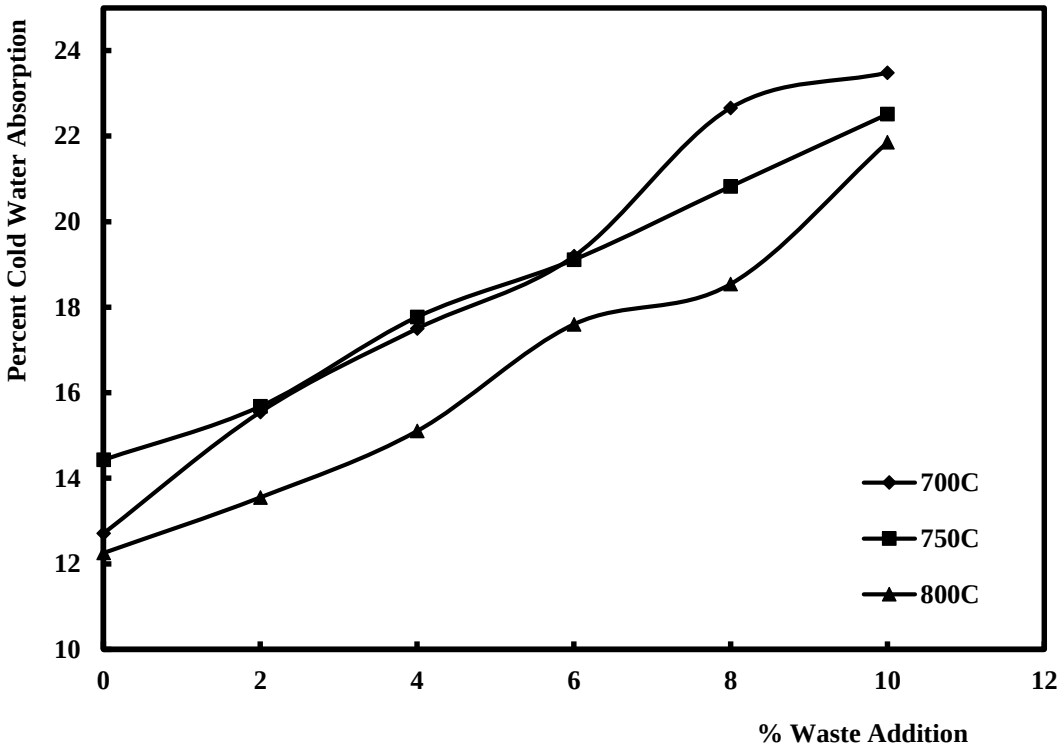

Fig (11) Effect of waste addition on percent cold water absorption

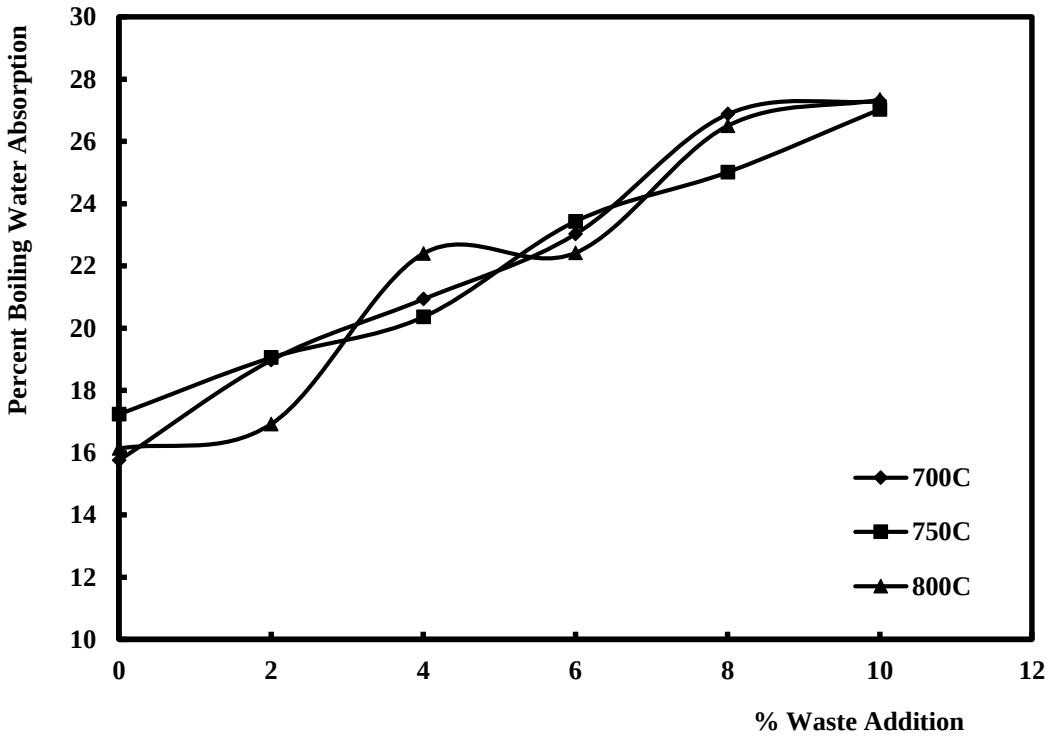

Fig (12) Effect of waste addition on percent boiling water absorption

As for the saturation coefficient, the effect of waste addition doesn't seem to affect the values of that parameter. However, Figure (13) reveals that the main parameter affecting that property is the firing temperature. The sintering process that becomes more serious at 800ºC causes a decrease in pore size resulting in lower values of saturation coefficient.

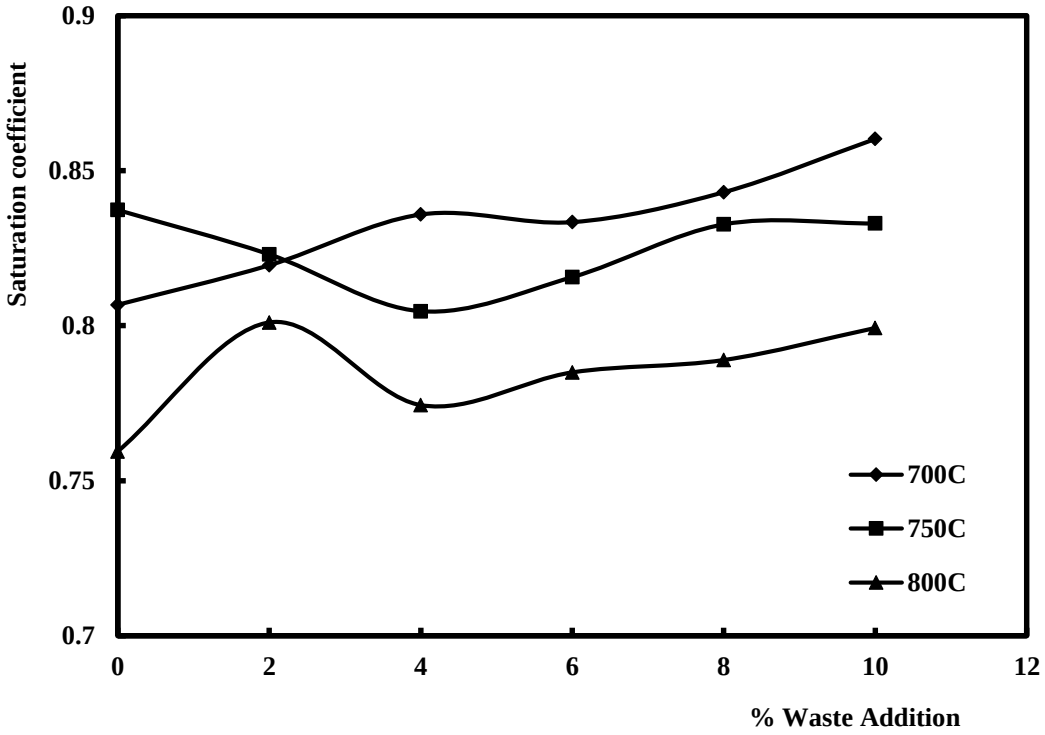

Fig (13) Effect of waste addition on saturation coefficient

3.3.4 Determination of Apparent Porosity and Bulk Density [ASTM C 373/1988 (Reapproved 2006)]

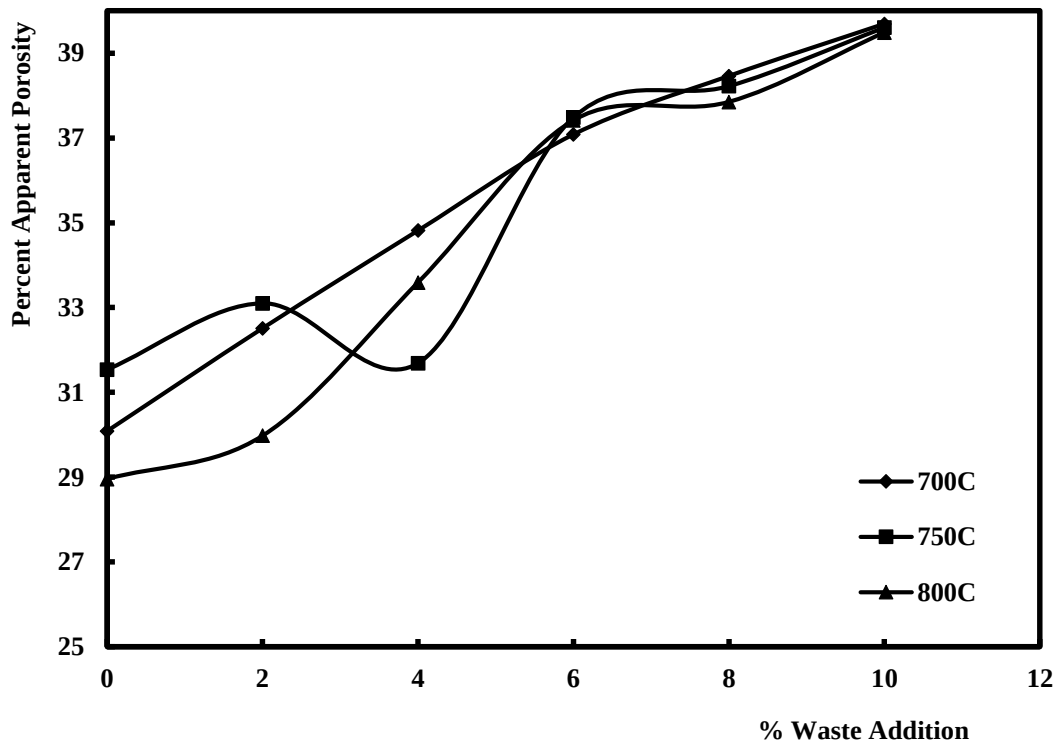

Fig (14) Effect of waste addition on apparent porosity

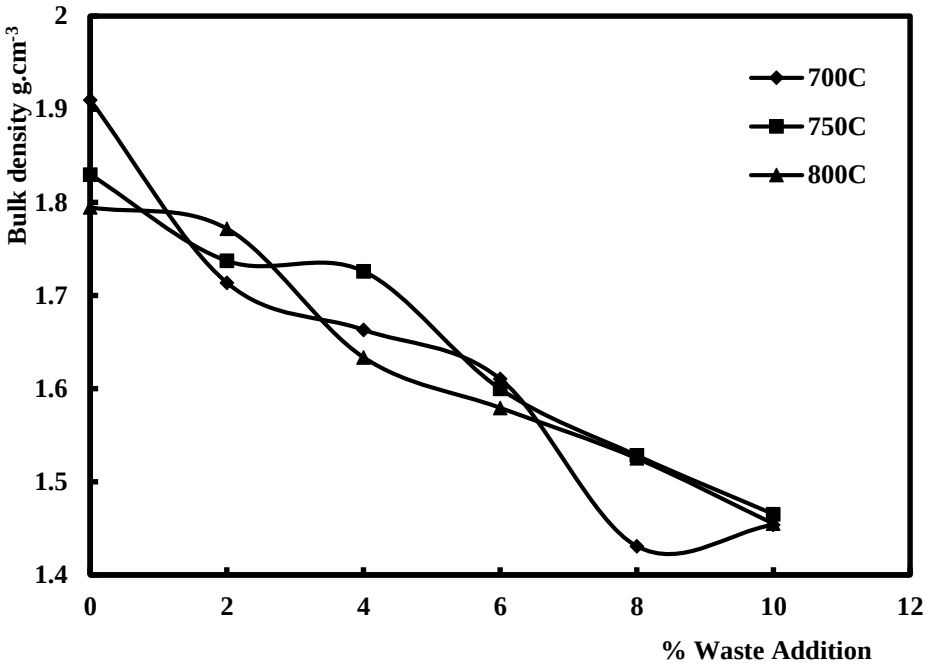

Fig (15) Effect of waste addition on bulk density

3.3.5 Determination of Compressive Strength

The effect of firing temperature on compressive strength is not remarkable whereas the addition of tanning waste causes a steady decrease in strength. In Figure (16) the values of strength are compared to the minimum allowable strength according to ASTM C62/2017 [32] (8.7MPa). It is clear that the waste can be added up to 5% level with a firing temperature as low as 700ºC.

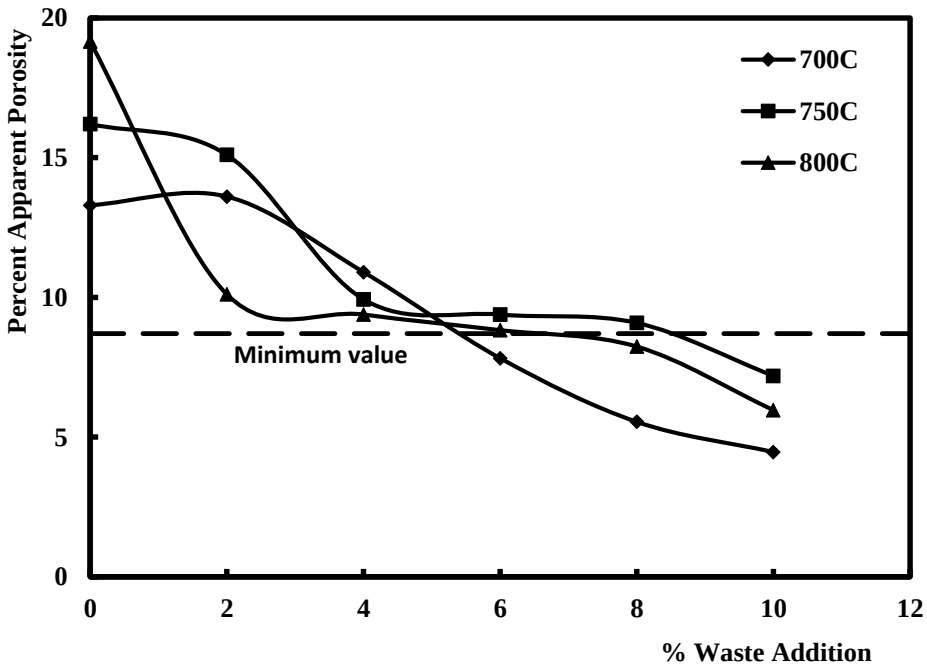

Fig (16) Effect of waste addition on compressive strength

The decrease in compressive strength following the addition of waste is related to the increase in porosity as can be followed from Figure (17) in which a power function can be fairly fitted between the two variables, following the suggestion of Gibson [33].

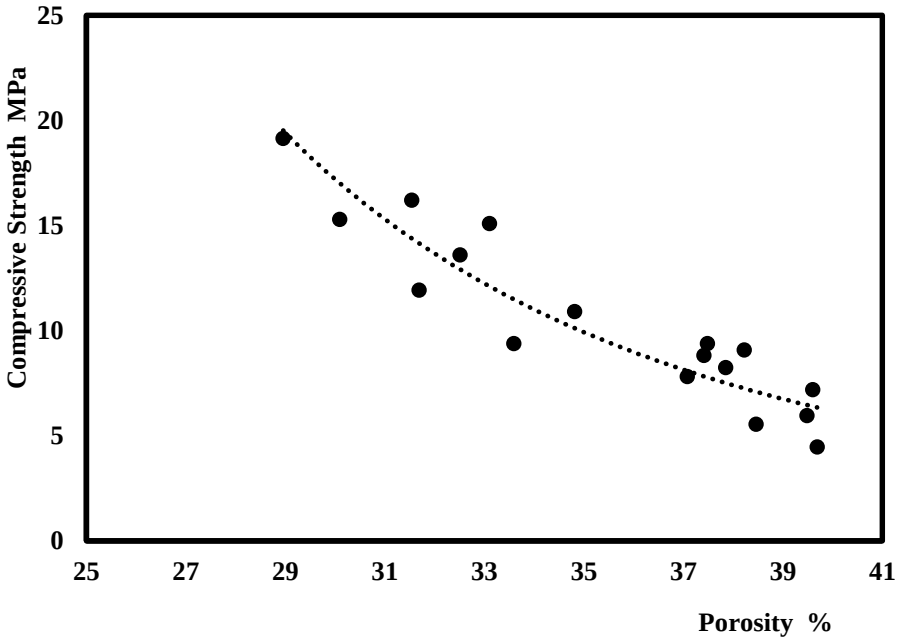

Fig (17) Dependence of compressive strength on porosity

4. CONCLUSIONS

Tannery powder obtained by drying sludge was used as additive to clay. Cubic brick molded by uniaxial pressure of 20KN force, with 15 % water addition. Drying and firing was performed for a soaking period of 1 hour and total firing time of 3 hours at 700°C, 750°C, and 800°C and heating rate close as possible to industrial conditions for clay brick samples. It is clear that the waste can beaadded up to 5% level with a firing temperature as low as 700ºC where the values of strength are compared to the minimum allowable strength according to ASTM C62/2017 (8.7MPa), furthermore decreasing in the weight of produced bricks. The use of waste sludge as addition to clay brick display economic and environmental advantages as it makes use of a polluting waste

REFERENCES

[1] Lynch, G.C.J. 1994, "Bricks: Properties and Classifications", Structural Survey, Vol. 12 Iss: 4, pp.15 – 20

[2] Dondi, M., Marsigli M. & Fabbri, B., 1997, "Recycling of industrial and urban wastes in brick production-A review", Tile & Brick International, 13 (3), pp 218-225

[3] Shakir A.A. and Mohammed A.A., "Manufacturing of Bricks in the Past, in the Present and in the Future", International Journal of Advances in Applied Sciences (IJAAS), 2 (3), 2013, pp. 145~156

[4] Crucido V.A. and cremades L.V. "Environmental effects of using clay bricks produced with sewage sludge: leachability and toxicity studies.", Waste Manag. 2012 Jun; 32(6): 1202-8

[5] Chemani H, and Chemani B. "Valorization of wood saw dust in making porous clay bricks", Sci. Res. Essays, April 2013, 8 (15), 609 – 614

[6] Demir I., Baspinar M, and Orhan M. "Utilization of kraft pulp production residues in clay brick production", Build. Environ. (2005) 40, 1533 - 1537

[7] Sutku M. and Akkurt S. "The use of recycling used paper residues in making porous bricks with reduced thermal conductivity" Ceram. Int. 35(7), 2009, 2625 - 2631

[8] Veiseh S., Yousefi A. A, "The use of polystyrene in lightweight brick production", Iran. Polym. J, 12,(4) 2003, 324-329,.

[9] Demir I. "An investigation on the production of construction bricks with processed waste tea" Build. Environ. (2006) 401, 1274 - 1277

[10] Abdul Kadir A. and Mohajerani A. "Density, strength, thermal conductivity and leachate characteristics of light weight clay bricks incorporating cigarette butts" Int. J. Civ. Environ. Eng. 2 (2010) 179 - 184

[11] Gorhan J. and Simsek O. "Porous clay bricks manufactured from rice husks" Const. Build. Mater. 40 (2013), 390 - 396

[12] Elwan M.M., Attriss M.S., Mahmoud A.A. and salem A.S. "Characterization of rice straw/ash and use in clay bricks" Proc. 1st Environ. Conf. (2006), Zagazig, Egypt

[13] Ajam L, Ouezdou M B, Felfoul H S and El Mensi R Characterization of the Tunisian phosphogypsu and its valorization in clay bricks. Constr. Build. Mater. (2009) 23: 3240–3247

[14] Ogila W.A. "Recycling of cement kiln dust in red clay

bricks and its impact on their physic-mechanical behavior" Int. J. Sci. Eng. Res. 5(2), 2014, 1072 – 1080

[15] UNIDO, 1998. Solidification and Stabilisation of Tannery Sludge. United Nations Industrial Development Organization, South - East asia.

[16] Juel M.A.I., Mizan A., Ahmed T. (2017) "Sustainable use of tannery sludge in brick manufacturing in Bangladesh" Waste Manag. 60: 259 – 269.

[17] Amsayazhi P., Mohan K.S.R. (2018) "Use of Sludge Waste as Ingredient in Making of Brick" Int. J. Eng. Tech. 7(3.12): 419 – 422

[18] Abadir M.F., Elements of ceramic technology‖ , 6th Edition, Faculty of Engineering, Cairo University, (2011).

[19] ICDD, Mineral powder diffraction file data book‖ , (sets 1-42), Pennsylvania, USA, (1993).

[20] Olphen H.V., Fripiat J.J., Data handbook for clay materials and other non–metallic minerals‖ , first edition, Pergamon Press Inc., New York, (1979), 243-284

[21] ASTM D 422 / 1963 (Reapproved 2007), "Method for particle–size analysis of soils", Annual book of American Society for Testing of Material (ASTM), U.S.A., 4(8), (March 2014).

[22] ASTM E 11 / 2009, "Specifications for wire–cloth sieves for testing purposes", Annual book of American Society for Testing of Material (ASTM), U.S.A., 14(2), (July 2013).

[23] Abadir M.F., "Mechanical unit operation of particulate solids", Cairo University, Faculty of Engineering Press, (2010).

[24] ASTM C 326/2009 (Reapproved 2018): Standard test method for drying and firing shrinkages of ceramic white- ware clays. ASTM Annual Book, U.S.A., 15 (2) (2017).

[25] ASTM C 67 / 2013, "Standard test methods for sampling and testing brick and structural clay tile", ASTM annual book, U.S.A., 4(5), (2017).

[26] ASTM D 7348 / 2008, "Standard test methods for loss on ignition (L.O.I) of solid combustion residues", Annual book of American Society for Testing of Material(ASTM), U.S.A., 5(6), (September 2013).

[27] ASTM C 373 / 1988 (Reapproved 2006), "Standard test method for water absorption, bulk density, apparent porosity, and apparent specific gravity of fired white ware products", Annual book of American Society for Testing of Material (ASTM), U.S.A., 15(2), (April 2014).

[28] Addala S., Bouhdjer L. Chala A., Bouhdher A. (2013) "Structural and optical properties of a NaCl single crystal doped with CuO nanocrystals" Chinese Phys. B 22(9): 1056 – 1088

[29] Abdel Razek E.M. (2007) "Influence of FeCl3 filler on the structure and physical properties of polyethyl-methacrylate films" Phys. B (Cond. Matter) 400(1-2): 31 – 36

[30] Mohassab Y. (2011) "Sulfur and phosphorus distribution between liquid iron and magnesia-saturated slag in hydrogen/water atmosphere relevant to a novel green iron making technology" MScThesis, The University of Utah, USA.

[31] Sarbatly R., Yee C.P., Fong T.S., Krishnaiah D. (2009) "Particle Size Distribution and Purification of Red Clay for Industrial Use". J. Appl. Sci., 9: 2344-2347

[32] ASTM C62/2017, "Standard Specification for Building Brick (Solid Masonry Units Made from Clay or Shale)", Annual book of American Society for Testing of Material (ASTM), U.S.A., 15(2), (April 2014).

[33] Gibson, L. J. (1989) 'Modelling the Mechanical Behavior of Cellular Materials. Mater. Sci. Eng., A A110: 1–36.